CROATICA CHEMICA ACTA
CCACAA, ISSN-0011-1643, ISSN-1334-417X

Croat. Chem. Acta **82** (2) (2009) 553–559
CCA-3345

Original Scientific Paper

Association of Nitrate Ion with Metal Cations in Aqueous Solution: a UV-Vis Spectrometric and Factor-Analytical Study*

Vlatka Gvozdić,[a] Vladislav Tomišić,[b,] Vjekoslav Butorac,[b] and Vladimir Simeon[b]**

[a]*Department of Chemistry, Josip Juraj Strossmayer University of Osijek, Franje Kuhača 20, 31000 Osijek, Croatia*
[b]*Laboratory of Physical Chemistry, Department of Chemistry, Faculty of Science, University of Zagreb, Horvatovac 102a, 10000 Zagreb, Croatia*

RECEIVED OCTOBER 14, 2008; ACCEPTED APRIL 2, 2009

Abstract. Ion association in aqueous solutions of varied concentrations of $LiNO_3$, $NaNO_3$, $Ca(NO_3)_2$, $Sr(NO_3)_2$, $Ba(NO_3)_2$, $Mn(NO_3)_2$, $Co(NO_3)_2$, $Ni(NO_3)_2$, $Cu(NO_3)_2$, $Zn(NO_3)_2$, and $Cd(NO_3)_2$ was studied by means of UV spectrometry. In all cases, except for $Zn(NO_3)_2(aq)$, the principal-components (PCA) and evolving-factor (EFA) analyses of the spectra indicated formation of associated ion pairs $[MNO_3]^{z-1}$ (M^z denotes the cation) at higher salt concentrations. The (dis)similarities of the $[MNO_3]^{z-1}$ spectral profiles (computed by EFA) were examined by means of cluster analysis. The influence of transition-metal ions on the nitrate UV spectrum was found to be remarkably different compared to that of non-transition cations. That could be a consequence of different types of cation-anion interactions. The ion pairs containing non-transition metal ions could be regarded as classical electrostatic ones, whereas a weak coordination interaction was presumably present in the ion pairs formed by the nitrate and the cations of transition metals.

Keywords: ion association, nitrate, UV spectrometry, principal components analysis, evolving factor analysis, cluster analysis

INTRODUCTION

The UV absorption spectrum of NO_3^- ion in aqueous solution is well known to contain two bands: a very strong one at ≈ 200 nm (assigned to $\pi^* \leftarrow \pi$ transition) and a much weaker one near 300 nm (assigned to $\pi^* \leftarrow n$ transition). The two bands are separated by a minimum near 260 nm.[1–5] It is also known that the $NO_3^-(aq)$ spectra are concentration-dependent, the concentration changes affecting the band positions as well as the band shapes.[1,4,6–8]

By applying factor-analytical methods to the UV spectra of $LiNO_3(aq)$ and $Co(NO_3)_2(aq)$ solutions at 25 °C, Tomišić and Simeon[4] concluded that the associated ion pairs, *viz.* $[LiNO_3]^0$ or $[CoNO_3]^+$, were formed at sufficiently high salt concentrations. Attempting to explain remarkable differences in the shapes of UV spectral bands of $LiNO_3(aq)$ and $Co(NO_3)_2(aq)$, they suggested that $[LiNO_3]^0$ should be similar to a classical (electrostatic) ion pair whereas $[CoNO_3]^+$ might be comparable to a coordination compound.

A recent study of temperature dependence of the nitrate UV bands has revealed the existence of a temperature-dependent equilibrium between two spectrally distinct 'free' nitrate species which were assumed to differ in the hydrogen-bonding structure of their hydration shells.[5,8,9] However, in the present work this equilibrium was not taken into account, since at working temperature (25 °C) most of the nitrate ions were in their 'low-temperature form'.[9]

Here we report on a study of the concentration dependence of UV-Vis absorption spectra of aqueous solutions of metal nitrates, $M^z(NO_3^-)_z$:

(*a*) cations of the main-group elements: $M^z = Li^+$, Na^+, Ca^{2+}, Sr^{2+}, Ba^{2+};

(*b*) transition-metal ions: $M^z = Mn^{2+}$, Co^{2+}, Ni^{2+}, Cu^{2+};

(*c*) post-transition metal ions: $M^z = Zn^{2+}$, Cd^{2+}.

Assuming that the associated ion pairs, $[MNO_3]^{z-1}$ are formed in sufficiently concentrated solutions, *i.e.*

* Dedicated to Professor Emeritus Drago Grdenić, Fellow of the Croatian Academy of Sciences and Arts, on the occasion of his 90th birthday.

** Author to whom correspondence should be addressed. (E-mail: vtomisic@chem.pmf.hr)

$$M^z(aq) + NO_3^-(aq) \rightleftarrows [M(NO_3)]^{z-1}(aq) \quad (1)$$

the spectral profiles, $\varepsilon(\lambda)$, of the solution species will be computed from the experimental spectrometric data by using the evolving factor analysis, EFA[10–12,13a] (ε denotes molar absorption coefficient). The (dis)similarities of the species' spectral profiles will be examined by visual inspection of the spectra and by means of cluster analysis.[14]

EXPERIMENTAL

All solid chemicals (originally of analytical reagent purity grade) were dried to constant mass and then dissolved in bidistilled water. For each of the examined electrolytes, a set of solutions was prepared, their concentrations ranging from $\lesssim$ 0.01 mol dm^{-3} to $\gtrsim$ 2 mol dm^{-3}. The absorption spectra of the solutions were recorded at (25.0 ± 0.1) °C by using a Varian Cary 5 UV-Vis-NIR double-beam spectrometer. The absorbances were sampled at 1 nm intervals. Parts of spectra where the absorbance exceeded ≈ 3.0 were discarded, for the sake of photometric accuracy. Complying with this condition, the wavelength range had to be limited to (230...350) nm.

COMPUTATIONS

The absorbances, A_{ij}, measured at the wavelengths λ_i (i = 1, 2, ... , I), in j-th solution (j = 1, 2, … , J; $J < I$) and divided by the length of optical path, l, were arranged into the data matrix:

$$\boldsymbol{A} = \left[a_{ij}\right] = \left[A_{ij} / l\right] \quad (2)$$

According to the Beer's law, the elements of $\boldsymbol{A}$ were defined as:

$$a_{ij} = \sum_{k=1}^{K} \varepsilon_{ik}\, c_{kj} \quad (3)$$

or, in matrix notation:

$$\boldsymbol{A} = \boldsymbol{E} \cdot \boldsymbol{C}^{\mathrm{eq}} \quad (4)$$

$K < J$ denotes the (unknown) number of UV-absorbing solute species, while $\boldsymbol{E}$ and $\boldsymbol{C}^{\mathrm{eq}}$ are (also unknown) matrices of molar absorption coefficients, ε, and species' concentrations, c, respectively.

Principal Components Analysis (PCA)

By singular value decomposition (SVD)[13b] of the data matrix one obtains:

$$\boldsymbol{A} = \boldsymbol{U} \cdot \boldsymbol{S} \cdot \boldsymbol{V}^{\mathrm{T}} \quad (5)$$

where $\boldsymbol{U}$ and $\boldsymbol{V}$ are row-orthogonal and column-orthogonal matrices, respectively, and $\boldsymbol{S}$ is a diagonal matrix containing singular values of $\boldsymbol{A}$:

$$\boldsymbol{S} = \mathrm{diag}(s_1 \geq s_2 \geq \ldots \geq s_K \geq \ldots \geq s_J) \quad (6)$$

Eq. (5) can be expanded into the sum of mutually orthogonal components:

$$\boldsymbol{A} = \sum_{j=1}^{J} \boldsymbol{A}_j = \sum_{j=1}^{J} \boldsymbol{u}_j \cdot s_j \cdot \boldsymbol{v}_j^{\mathrm{T}} \quad (7)$$

The relative importance of a component is indicated by the magnitude of the corresponding singular value.

Due to inevitable experimental errors, the $\boldsymbol{A}$ matrix has a full rank of J. However, owing to the orthogonality of $\boldsymbol{U}$ and $\boldsymbol{V}$, all chemically relevant information is contained in K first components (having the highest singular values) which are called *principal components*. The remaining components contain nothing but the experimental (mostly random) error. Since each principal component ($\tilde{\boldsymbol{A}}_k$, say) is positively correlated with the experimental data, its significance can be checked by means of a statistical test on the R_0 statistic:[15]

$$R_0(k) = \sqrt{s_k^2 \Big/ \sum_{m=1}^{J} s_m^2} \quad (8)$$

(k = 1, 2, ...). The estimated number of principal components, K, is usually called the pseudorank or effective rank of $\boldsymbol{A}$. In the present context, it is interpreted as the number of spectrally distinguishable chemical species.

Evolving Factor Analysis (EFA)

The unknown matrices $\boldsymbol{E}$ and $\boldsymbol{C}$ cannot be computed from the results of PCA alone, some additional information is needed. Since the extent of ion association monotonically increases with increasing salt concentration, it follows that in the cases considered here the total salt concentration, c, can serve as an 'evolution variable' which defines the order of the spectra in the data matrix. Therefore, the evolving factor analysis, EFA,[10–12,13a] was used in subsequent analyses of speciation.

The initial stage of analysis ('forward EFA') consists of successive SVDs of a series of submatrices of $\boldsymbol{A}$ containing the *first* j columns (j = 1, 2, 3, ..., J). The obtained log s_j values are then normalised by dividing by Σ_j log s_j, and plotted against c_j. In the next stage ('reverse EFA'), the successive submatrices are formed from the *last* j (j = 1, 2, 3, ..., J) columns of $\boldsymbol{A}$, the rest of the computational procedure being analogous to that in forward EFA. If only two or three species are expected (as is the case here), the assignment of 'forward' and 'reverse' curves to the solute species, is elementary.

The final stage is an iterative least-squares refinement, aimed at obtaining consistent estimates of $\boldsymbol{E}$ and $\boldsymbol{C}$:

$$\tilde{\boldsymbol{E}}(n) = \boldsymbol{A} \cdot \tilde{\boldsymbol{C}}^{\mathrm{T}}(n) \cdot \left[\tilde{\boldsymbol{C}}(n) \cdot \tilde{\boldsymbol{C}}^{\mathrm{T}}(n) \right]^{-1} \quad (9)$$

$$\tilde{\boldsymbol{C}}(n) = \left[\tilde{\boldsymbol{E}}^{\mathrm{T}}(n) \cdot \tilde{\boldsymbol{E}}(n) \right]^{-1} \cdot \tilde{\boldsymbol{E}}^{\mathrm{T}}(n) \cdot \boldsymbol{A} \quad (10)$$

(the estimated quantities are denoted by superscribed tilde and n denotes the iteration number: $n = 1, 2, ...$). In each iteration cycle concentration profiles are normalised to the total concentrations, and all negative ε values and concentrations are set to zero. The final expression can be written as:

$$\tilde{\boldsymbol{A}}(K) = \tilde{\boldsymbol{E}}(K) \cdot \tilde{\boldsymbol{C}}(K) \quad (11)$$

The details can be found elsewhere.[4,16]

Cluster Analysis

Besides visual inspection of the positions and intensities of absorption maxima and minima, the spectra were examined by hierarchical cluster analysis.[14] Since each spectrum can be represented by a point in I-dimensional space, the Euclidean distance of two representing points can be taken as an indicator of dissimilarity of the two spectra under consideration (α and β, say):

$$d_{\alpha,\beta} = \sqrt{\sum_{i=1}^{I} (a_{\alpha,i} - a_{\beta,i})^2} \quad (12)$$

An agglomerative single-linkage ('nearest-neighbour') algorithm[14] was used: the analysis begins by combining two nearest representative points (A and B, say) into a single point (AB) and computing its distance from the initial point. In the next step, the nearest neighbour of AB is identified and combined with AB into the next 'cluster' (ABC). The procedure is repeated until all objects (spectra) are merged into a single cluster. The results obtained by hierarchical clustering are usually presented in the form of dendrograms.

RESULTS AND DISCUSSION

The UV absorption spectra of four systems investigated, namely $Ca(NO_3)_2$(aq), $Cd(NO_3)_2$(aq), $Mn(NO_3)_2$ (aq), and $Cu(NO_3)_2$(aq), are displayed in Figure 1 as representative examples.

Characteristic Spectral Shifts and Spectral Profiles of Solute Species

In all cases considered here, the positions of absorbance maxima were found to depend on the total salt concentration, c. These concentration-induced band shifts can be defined as:

$$\Delta\lambda = \lambda(c_2) - \lambda(c_1) \quad (13)$$

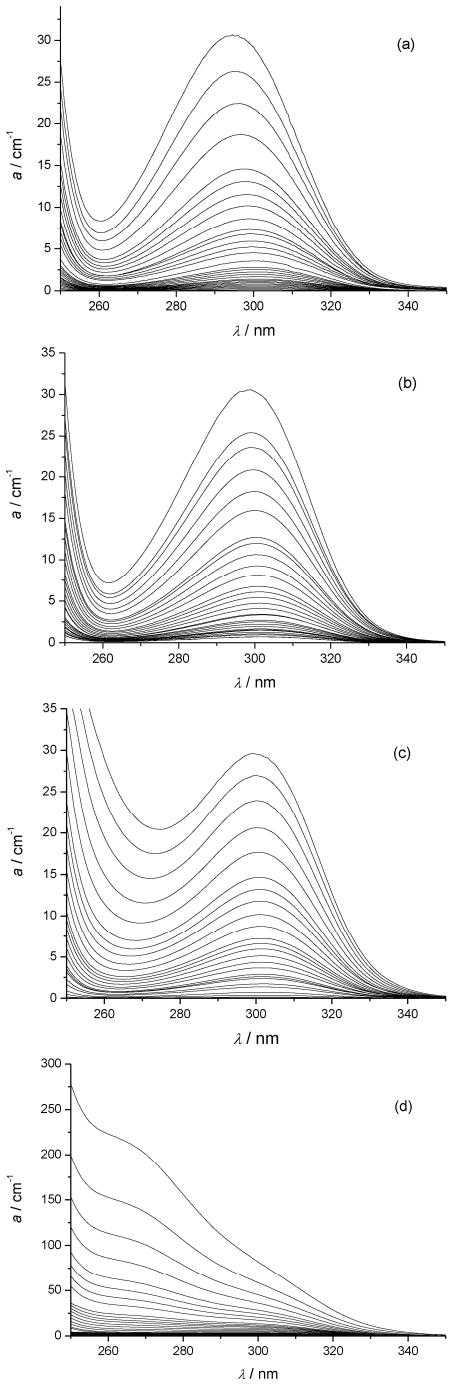

Figure 1. UV absorption spectra of: (a) $Ca(NO_3)_2$(aq), c = (0.01…2.0) mol dm^{-3}, l = 1 cm, 1 mm; (b) $Cd(NO_3)_2$ (aq), c = (0.01…2.4) mol dm^{-3}, l = 1 cm, 1 mm; (c) $Mn(NO_3)_2$(aq), c = (0.01...2.0) mol dm^{-3}, l = 1 cm, 1 mm; (d) $Cu(NO_3)_2$(aq), c = (0.0005…2.0) mol dm^{-3}, l = 10 cm, 1 cm, 1 mm, 0.1 mm. $a = A/l$.

c_1 and c_2 denoting the initial and final salt concentration, respectively. As can be seen from Table 1, the maxima were slightly shifted towards lower wavelengths (-8 nm $\leq \Delta\lambda_{\max} \leq -1$ nm).

Table 1. UV absorption spectra of aqueous solutions of metal nitrates, $M(NO_3)_z$: concentration-induced changes of positions of absorption maxima and minima and the number of UV absorbing species, N_{spec}

Solute	c_1 / mol dm^{-3}	c_2 / mol dm^{-3}	$\lambda_{max}(c_1)$ / nm	$\lambda_{max}(c_2)$ / nm	$\Delta\lambda_{max}$ [(a)] / nm	$\lambda_{min}(c_1)$ / nm	$\lambda_{min}(c_2)$ / nm	$\Delta\lambda_{min}$ [(a)] / nm	N_{spec}
$LiNO_3$	0.08	4.0	301	300	–1	262	261	–1	2
$NaNO_3$	0.01	4.0	302	300	–2	263	262	–1	2
$Ca(NO_3)_2$	0.01	2.0	302	294	–8	262	260	–2	2
$Sr(NO_3)_2$	0.01	1.8	302	295	–7	263	261	–2	2
$Ba(NO_3)_2$	0.01	0.3	302	299	–3	263	262	–1	2
$Mn(NO_3)_2$	0.01	2.0	302	299	–3	263	275	+12	2
$Co(NO_3)_2$	0.01	2.0	303	298	–5	263	274	+11	2
$Ni(NO_3)_2$	0.005	2.0	302	300	–2	262	266	+4	2
$Cu(NO_3)_2$	0.0005	0.2[(b)]	301	295	–6	267	284	+17	2
$Zn(NO_3)_2$	0.015	2.0	302	300	–2	263	263	0	1
$Cd(NO_3)_2$	0.01	2.4	302	300	–2	263	263	0	2

[(a)] $\Delta\lambda = \lambda(c_2) - \lambda(c_1)$
[(b)] Positions of minimum and maximum could not be determined at concentrations higher than 0.2 mol dm^{-3}.

The patterns of the shifts of absorbance minima, however, proved to be different: $\Delta\lambda_{min}$ values for the nitrates of non-transition cations (Li^+, Na^+, Ca^{2+}, Sr^{2+}, Ba^{2+}, Zn^{2+}, Cd^{2+}) were small non-positive numbers (–2 nm $\leq \Delta\lambda_{min} \leq$ 0), whereas $\Delta\lambda_{min}$ values for transition cations (Mn^{2+}, Co^{2+}, Ni^{2+}, Cu^{2+}) were all positive and appreciably larger, except for Ni^{2+}.

In most cases, both PCA and EFA indicated the presence of *two* UV absorbing species (see the last column of Table 1). Obviously, one of the two species should be the 'free' nitrate ion, NO_3^-(aq), the other being, in all probability, the associated ion pair, $[M(NO_3)(aq)]^{z-1}$ (M^z denotes the cation). The exceptions were the solutions of $Zn(NO_3)_2$, where only one species could be detected. The spectral profiles, $\varepsilon(\lambda)$, of NO_3^-(aq), and $[M(NO_3)(aq)]^{z-1}$ species, computed by means of EFA, are depicted in Figures 2 and 3.

The observed differences in concentration-induced spectral shifts (Figure 1, Table 1) and in the absorption spectra of associated species (Figures 2 and 3, Table 2) are in accordance with our previous assumption that the interactions within ion pairs containing cations with

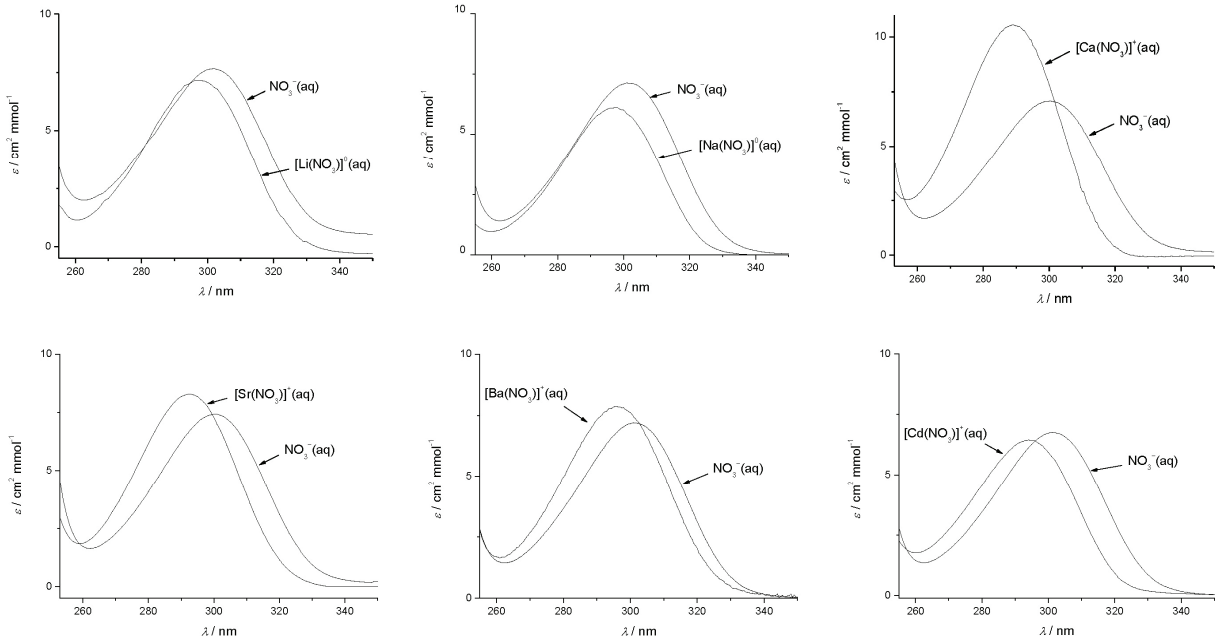

Figure 2. EFA results: UV absorption spectra of $[M(NO_3)_2]^{z-1}$(aq) species, compared to the spectrum of NO_3^-(aq); M^z = Li^+, Na^+, Ca^{2+}, Sr^{2+}, Ba^{2+}, Cd^{2+}.

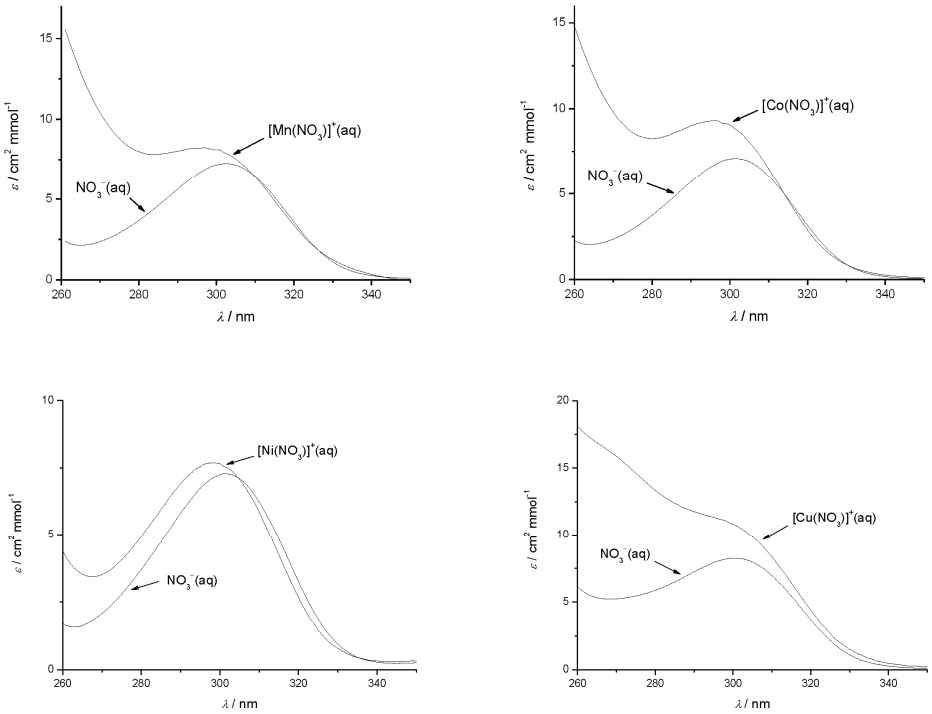

Figure 3. EFA results: UV absorption spectra of $[M(NO_3)_2]^{z-1}(aq)$ species, compared to the spectrum of $NO_3^-(aq)$ $M^z = Mn^{2+}$, Co^{2+}, Ni^{2+}, Cu^{2+}.

noble-gas electron configuration could be regarded to be purely electrostatic, whereas a weak coordination interaction may be present in the ion pairs of nitrate and transition-metal cations.[4] Having that in mind, one would expect the effect of post-transition metal cations (completely filled *d* orbitals) on the nitrate UV bands to be more similar to that of alkali and alkaline earth metal ions as compared to divalent transition-metal ions. Indeed, the data presented in Tables 1 and 2 and in Figures 1–3 confirm this expectation. As already mentioned, PCA of the $Zn(NO_3)_2(aq)$, UV spectral matrix indicated a pseudorank of 1, *i.e.* no ion pairing could be detected. The same was observed earlier in the case of $Mg(NO_3)_2(aq)$ solutions, and explained to be the consequence of a strong hydration of Mg^{2+} ion.[4] Comparison of ionic radii of Zn^{2+} (0.74 Å, coordination

Table 2. EFA results: UV absorption spectra of $[M(NO_3)]^{z-1}(aq)$ species, compared to the spectrum of $NO_3^-(aq)$; $M^z = Li^+$, Na^+, Ca^{2+}, Sr^{2+}, Ba^{2+}, Cd^{2+}

Species	$\lambda_{max}(NO_3^-)$ / nm	$\lambda_{max}(MNO_3^{z-1})$ / nm	$\Delta\lambda_{max}$ [(a)] / nm	$\Delta\lambda_{min}$ [(a)] / nm	ε_{max} [(b)] / $cm^2\ mmol^{-1}$
$LiNO_3$	302	298	–4	–3	7.2...7.0
$NaNO_3$	301	298	–3	–3	7.1...6.1
$Ca(NO_3)_2$	301	289	–12	–6	7.1...10.4
$Sr(NO_3)_2$	301	293	–8	–3	7.3...10.3
$Ba(NO_3)_2$	301	296	–5	–2	7.1...7.7
$Mn(NO_3)_2$	302	297	–5	+19	7.3...8.0
$Co(NO_3)_2$	301	296	–5	+16	7.1...8.9
$Ni(NO_3)_2$	302	297	–5	+5	7.2...7.7
$Cu(NO_3)_2$	301	[(c)]	[(c)]	[(c)]	8.2...[(c)]
$Cd(NO_3)_2$	301	294	–7	–3	6.8...6.4

[(a)] $\Delta\lambda = \Delta\lambda(MNO_3^{z-1}) - \lambda(NO_3^-)$
[(b)] Values for $NO_3^-(aq)$ and $[M(NO_3)]^{z-1}(aq)$
[(c)] The spectrum of $[Cu(NO_3)]^+$ has no maxima or minima in the examined wavelength range.

number 6) and Mg^{2+} (0.72 Å, coordination number 6)[17] suggests that the same reasoning can be applied to the $Zn(NO_3)_2$ aqueous solutions.

It should be noted that among the first-row transition-metal cations examined, the effect of Cu^{2+} on the nitrate UV spectrum is remarkably the largest (Figure 1, Table 1). That could be explained by the well known Jahn-Teller distortion of the (elongated) octahedral $[Cu(H_2O)_6]^{2+}$ complex. Due to this distortion the axial water molecules are loosely bound to the central metal ion and can be rather easily substituted by NO_3^- ion. Another peculiarity of the UV spectra of concentrated $Cu(NO_3)_2(aq)$ solutions is the appearance of a shoulder centered at approximately 265 nm (Figures 1 and 2) which could be assigned to the charge transfer from the nitrate to the copper(2+) ion.[6,18]

The magnitudes of nitrate UV spectrum shifts caused by Mn^{2+} and Co^{2+} are similar, whereas the corresponding influence exerted by Ni^{2+} in the same $M(NO_3)_2$ concentration range is considerably less pronounced (Table 1). The latter finding can be accounted for by the fact that, among the high-spin octahedral hexaaqua complexes of the first-row transition-metal divalent cations, $[Ni(H_2O)_6]^{2+}$ has the highest crystal field stabilization energy as well as the highest absolute value of hydration enthalpy.[19] The displacement of the water molecules by NO_3^- should therefore be energetically less favourable in the case of $Ni^{2+}(aq)$ than for the other transition cations examined. Consequently, that is reflected in the relatively weak concentration dependence of UV spectra of $Ni(NO_3)_2(aq)$ solutions.

Cluster Analysis

A dendrogram obtained by cluster analysis of associated ion pairs spectra (see Figures 2 and 3) is shown in Figure 4.

At higher distances three clusters can be observed: a single-member cluster corresponding to Cu^{2+}, a two-member cluster containing Mn and Cu, and a complex eight-member cluster which at lower distances splits into clusters which comprise the remaining cations examined (Ca^{2+}, Sr^{2+}, Ba^{2+}, Li^{+}, Na^{+}, Cd^{2+}, Ni^{2+}). Thus, the results of cluster analysis are in agreement with the considerations stated above (based on visual inspection of the spectra), and can be taken to additionally corroborate the assumption that different types of interactions exist in the ion pairs of nitrate with transition- and non-transition metal ions.

Acknowledgement. This work was supported by the Ministry of Science, Education and Sports of the Republic of Croatia (Project No. 119-1191342-2960).

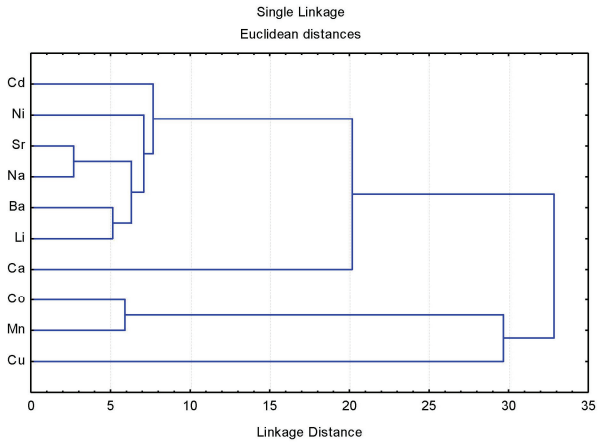

Figure 4. Dissimilarities (see Eq. (12)) of the spectra of $[M(NO_3)]^{z-1}(aq)$ species containing different cations; M^z = Li^+, Na^+, Ca^{2+}, Sr^{2+}, Ba^{2+}, Mn^{2+}, Co^{2+}, Ni^{2+}, Cu^{2+}, Cd^{2+}.

REFERENCES

1. D. Mayerstein and A. Treinin, *Trans. Faraday Soc.* **57** (1961) 2104–2112.
2. A. Mookherji and S. P. Tandon, *Indian J. Phys.* **36** (1962) 211–212.
3. A. Mookherji and S. P. Tandon, *Indian J. Phys.* **36** (1962) 344–350.
4. V. Tomišić and Vl. Simeon, *Phys. Chem. Chem. Phys.* **1** (1999), 299–302.
5. V. Tomišić, V. Butorac, J. Viher, and Vl. Simeon, *J. Solution Chem.* **34** (2005) 613–616.
6. B. J. Hathaway and A. E. Underhill, *J. Chem. Soc.* (1962) 2257–2262.
7. E. Ivana and E. Popa, *Rev. Roum. Chim.* **12** (1967) 541–546.
8. V. Butorac, Vl. Simeon, and V. Tomišić, *Croat. Chem. Acta.* **80** (2007) 533–539.
9. Vl. Simeon, V. Butorac, V. Tomišić, and N. Kallay, *Phys. Chem. Chem. Phys.* **5** (2003) 2015–2019.
10. H. Gampp, M. Maeder, C. J. Meyer, and A. D. Zuberbühler, *Talanta* **32** (1985) 1133–1139.
11. H. Gampp, M. Maeder, C. J. Meyer, and A. D. Zuberbühler, *Chimia* **39** (1985) 315–317.
12. H. Gampp, M. Maeder, C. J. Meyer, and A. D. Zuberbühler, *Talanta* **33** (1986) 943–951.
13. E. R. Malinowski, *Factor Analysis in Chemistry*, 3rd ed., Wiley, New York, 2002, (a) pp. 160–166, (b) pp. 51–52.
14. B. G. M. Vandeginste, D. L. Massart, L. M. C. Buydens, S. de Jong, P. J. Lewi, and J. Smeyers-Verbeke, *Handbook of Chemometrics and Qualimetrics*, Part B, Elsevier, Amsterdam 1998, pp. 57–86.
15. D. Pavković, V. Tomišić, R. Nuss, and Vl. Simeon, *Croat. Chem. Acta* **69** (1996) 1175–1188.
16. V. Tomišić and Vl. Simeon, *Phys. Chem. Chem. Phys.* **2** (2000) 1943–1949.
17. D. R. Lide (Ed.), *CRC Handbook of Chemistry and Physics*, 82nd ed., CRC Press, Boca Raton, FL, 2001, pp. **12**–15 and **12**–16.
18. C. C. Addison and D. Sutton, *J. Chem. Soc.* (1966) 1524–1528.
19. J. Burgess, *Metal Ions in Solution*, Ellis Horwood Ltd., Chichester 1978, pp. 182–184.

SAŽETAK

Asocijacija nitratnog iona s metalnim kationima u vodenim otopinama: UV-Vis spektrometrijsko i faktorsko-analitičko istraživanje

Vlatka Gvozdić,[a] Vladislav Tomišić,[b] Vjekoslav Butorac[b] i Vladimir Simeon[b]

[a]*Odjel za kemiju, Sveučilište Josipa Jurja Strossmayera u Osijeku, Franje Kuhača 20, 31000 Osijek, Hrvatska*

[b]*Zavod za fizikalnu kemiju, Kemijski odsjek, Prirodoslovno-matematički fakultet, Sveučilište u Zagrebu, Horvatovac 102a, 10000 Zagreb, Hrvatska*

Asocijacija iona u vodenim otopinama $LiNO_3$, $NaNO_3$, $Ca(NO_3)_2$, $Sr(NO_3)_2$, $Ba(NO_3)_2$, $Mn(NO_3)_2$, $Co(NO_3)_2$, $Ni(NO_3)_2$, $Cu(NO_3)_2$, $Zn(NO_3)_2$, i $Cd(NO_3)_2$ proučavana je UV-Vis spektrometrijom. Analizom glavnih komponenata (PCA) i evolucijskom faktorskom analizom (EFA) u svim je slučajevima, osim $Zn(NO_3)_2(aq)$, pri višim koncentracijama soli utvrđeno nastajanje asociranih ionskih parova $[MNO_3]^{z-1}$ (M^z označuje kation). Sličnosti i razlike spektara vrsta $[MNO_3]^{z-1}$ (izračunanih primjenom EFA) istražene su metodom rojne analize. Utvrđeno je da je utjecaj iona prijelaznih metala na UV spektar nitrata bitno različit od učinka alkalijskih, zemnoalkalijskih ili postprijelaznih kationa, što se može protumačiti različitim vrstama međudjelovanja kation-anion. Ionski parovi koji sadrže katione neprijelaznih metala mogu se smatrati klasičnim, elektrostatskim parovima, dok je u asocijata kationa prijelaznih metala i nitrata vjerojatno prisutna slaba koordinacijska interakcija.